Reprogrammed transsulfuration promotes basal-like breast tumor progression via realigning cellular cysteine persulfidation

Katalin Erdélyi[a,1], Tamás Ditrói[a,1], Henrik J. Johansson[b], Ágnes Czikora[a], Noémi Balog[a], Laxmi Silwal-Pandit[c], Tomoaki Ida[d], Judit Olasz[e], Dorottya Hajdú[a], Zoltán Mátrai[f], Orsolya Csuka[e], Koji Uchida[g], József Tóvári[h], Olav Engebraten[i], Takaaki Akaike[d], Anne-Lise Børresen Dale[c], Miklós Kásler[j], Janne Lehtiö[b], and Péter Nagy[a,k,l,2]

[a]Department of Molecular Immunology and Toxicology, National Institute of Oncology, 1122 Budapest, Hungary; [b]Science for Life Laboratory, Department of Oncology-Pathology, Karolinska Institutet, 171 21 Solna, Sweden; [c]Department of Cancer Genetics, Institute for Cancer Research, Oslo University Hospital, N-0379 Oslo, Norway; [d]Department of Environmental Medicine and Molecular Toxicology, Tohoku University Graduate School of Medicine, Sendai 980-8575, Japan; [e]Department of Pathogenetics, National Institute of Oncology, 1122 Budapest, Hungary; [f]Department of Surgery, National Institute of Oncology, 1122 Budapest, Hungary; [g]Department of Applied Biological Chemistry, Graduate School of Agricultural and Life Sciences, University of Tokyo, Tokyo 113-8657, Japan; [h]Department of Experimental Pharmacology, National Institute of Oncology, 1122 Budapest, Hungary; [i]Department of Oncology, Faculty of Medicine, Institute for Cancer Research, Oslo University Hospital, University of Oslo, 0372 Oslo, Norway; [j]Department of Head and Neck Surgery, National Institute of Oncology, 1122 Budapest, Hungary; [k]Department of Anatomy and Histology, University of Veterinary Medicine, 1078 Budapest, Hungary; and [l]Institute of Oncochemistry, University of Debrecen, 4012 Debrecen, Hungary

Edited by Solomon H. Snyder, Johns Hopkins University School of Medicine, Baltimore, MD, and approved September 29, 2021 (received for review January 3, 2021)

Basal-like breast cancer (BLBC) is the most aggressive subtype of breast tumors with poor prognosis and limited molecular-targeted therapy options. We show that BLBC cells have a high Cys demand and reprogrammed Cys metabolism. Patient-derived BLBC tumors from four different cohorts exhibited elevated expression of the transsulfuration enzyme cystathione β-synthetase (CBS). CBS silencing (shCBS) made BLBC cells less invasive, proliferate slower, more vulnerable to oxidative stress and cystine (CySSCy) deprivation, prone to ferroptosis, and less responsive to HIF1-α activation under hypoxia. shCBS xenograft tumors grew slower than controls and exhibited impaired angiogenesis and larger necrotic areas. Sulfur metabolite profiling suggested that realigned sulfide/persulfide-inducing functions of CBS are important in BLBC tumor progression. Supporting this, the exclusion of serine, a substrate of CBS for producing Cys but not for producing sulfide/persulfide, did not exacerbate CySSCy deprivation–induced ferroptosis in shCBS BLBC cells. Impaired Tyr phosphorylation was detected in shCBS cells and xenografts, likely due to persulfidation-inhibited phosphatase functions. Overexpression of cystathione γ-lyase (CSE), which can also contribute to cellular sulfide/persulfide production, compensated for the loss of CBS activities, and treatment of shCBS xenografts with a CSE inhibitor further blocked tumor growth. Glutathione and protein-Cys levels were not diminished in shCBS cells or xenografts, but levels of Cys persulfidation and the persulfide-catabolizing enzyme ETHE1 were suppressed. Finally, expression of enzymes of the oxidizing Cys catabolism pathway was diminished, but expression of the persulfide-producing CARS2 was elevated in human BLBC tumors. Hence, the persulfide-producing pathways are major targetable determinants of BLBC pathology that could be therapeutically exploited.

persulfide | transsulfuration | hydrogen sulfide | basal-like breast cancer | cystathione β-synthetase

The prediction of prognosis and treatment responsiveness by molecular stratification of breast cancer patients based on Perou et al.'s 50 identified transcripts is still a widely used clinical practice (1). Out of the five designated PAM50 subgroups from this study, the basal-like breast cancer (BLBC) subtype (representing ∼15% of patients) encompasses the most aggressive breast tumors and the poorest prognosis. A characteristic feature of this subtype is the lack of hormone receptors for estrogen (ER) and progesterone (PR) and human epidermal growth factor receptor-2 (HER2) and are hence denominated "triple-negative" cancers, which renders therapies targeting these receptors ineffective. Therefore, a better understanding of the underlying biological characteristics of BLBC is essential to devising novel molecular stratagems to widen the scope of medical oncology interventions, which currently rely predominantly on classical chemotherapies for BLBC patients.

The cellular reprogramming of metabolic pathways to aid tumor progression is a featured hallmark of most cancers (2, 3). Consequently, recognized vulnerabilities of cancer cells to particular metabolic pathways represent a major focus in current drug development endeavors (4). Recent studies (5, 6) demonstrated that carcinogenic rewiring of the metabolism of the nonessential amino acid cysteine (Cys) can support cancer cell growth (6). Cys residues in proteins and in glutathione

Significance

Basal-like breast cancers (BLBC) have poor prognosis. Here, we present evidence that reprogrammed transsulfuration is a hallmark of BLBC. Human BLBC tumors exhibit elevated levels of cystathione β-synthetase (CBS) but diminished expressions of oxidative Cys-catabolizing enzymes supporting a Cys-addicted phenotype. We demonstrated that in BLBC cells, CBS plays a role in cellular proliferation and invasiveness, HIF1-α activation under hypoxia, and protection against oxidative stress and CySSCy deprivation–induced ferroptosis. Tumor progression and angiogenesis was impaired in shCBS xenograft tumors, which had larger intratumoral necrotic areas. Mechanistic analyses largely based on sulfur metabolome and proteomics data revealed that realigned Cys persulfidation is a determining factor in this Cys-addicted phenotype of BLBC tumors, which holds promise for drug development.

Author contributions: P.N. designed research; K.E., T.D., H.J.J., Á.C., N.B., L.S.-P., T.I., J.O., D.H., O.C., J.T., O.E., T.A., and J.L. performed research; K.U. contributed new reagents/analytic tools; K.E., T.D., H.J., Á.C., L.S.-P., T.I., Z.M., J.T., O.E., T.A., A.-L.B.D., M.K., J.L., and P.N. analyzed data; Z.M., A.-L.B.D., and M.K. provided essential intellectual input; P.N. conceived and oversaw the study; and K.E., T.D., and P.N. wrote the paper.

The authors declare no competing interest.

This article is a PNAS Direct Submission.

[1]K.E. and T.D. contributed equally to this work.

[2]To whom correspondence may be addressed. Email: peter.nagy@oncol.hu.

This article contains supporting information online at http://www.pnas.org/lookup/suppl/doi:10.1073/pnas.2100050118/-/DCSupplemental.

Published November 5, 2021.

(GSH) are critical primary targets of reactive oxygen species (ROS) and play major roles in antioxidant protection and redox regulation of cellular signaling and metabolism (7–10). Importantly, susceptibility to oxidative stress is another well-studied liability of most cancer cells (11–13).

Cells can effectively take up the oxidized disulfide–linked dimeric form of Cys, namely cystine (CySSCy), from extracellular fluids via the glutamate-CySSCy antiporter (xCT), which due to its pivotal functions in cancer cell survival is an identified drug target (e.g., ref. 14). Tang et al. showed that BLBC cells rely on CySSCy supplementation in the culture medium to assure adequate GSH production for countering endogenous ROS-induced necrotic cell death (15). Alternatively, some cells can synthesize Cys de novo using serine (Ser) and the reduced sulfur derived from methionine (Met) via the transsulfuration pathway (16). It has recently been reported that under low exogenous CySSCy conditions, as is common in tumor interstitial fluids (17), the transsulfuration machinery becomes an essential source of Cys-sustaining GSH levels (6). Furthermore, decreased CySSCy uptake through xCT was linked to the methionine (Met)–dependent phenotype of breast cancer cells because under these conditions, the majority of Met via homocysteine (HCys) is used for Cys production, leading to impaired remethylation (18). These studies clearly underline the importance of an adequate Cys supply for BLBC cell growth and forecast a fine-tuned crosstalk between its uptake from exogenous sources and its intracellular production.

In recent years, the cancer cell–protecting functions of the transsulfuration enzymes cystathione β-synthetase (CBS) and cystathione γ-lyase (CSE) were also highlighted in relation to their reverse transsulfuration activities to produce hydrogen sulfide (H_2S). H_2S is emerging as a versatile small signaling molecule in various organ systems, and recognition of its promiscuous roles in human pathologies, including cancer, is gaining ground (19–21). Driving protein functions via persulfidation of regulatory and catalytic Cys residues is one of the featured molecular models behind H_2S-mediated biological functions (22). Because this chemistry also occurs on Cys thiols, it is not surprising that persulfidation is tightly linked to redox-based events (23–25). Cys persulfides can also be generated without the direct involvement of H_2S via alternative enzymatic activities of CSE and CBS (24, 26) or 3-mercaptopyruvate sulfurtransferase (MPST) (27). Furthermore, we recently discovered that a moonlighting activity of cysteinyl–transfer RNA (tRNA) synthases (CARS) can produce large amounts of Cys persulfides and translationally incorporate these into nascent polypeptide chains (28). Although the intracellular prevalence and enzyme regulatory functions of protein-Cys persulfidation is now well documented (29, 30), the specific roles of sulfur metabolic pathways in producing persulfides under different pathophysiological conditions need further clarification. We demonstrated that the NADPH-driven disulfide-reducing machineries, the thioredoxin (Trx) and glutathione (GSH) systems, are the primary enzymes regulating endogenous persulfide homeostasis as well as persulfidation-mediated enzyme functions (29, 31). Furthermore, our recent study on the antioxidant and redox-signaling properties of persulfides led us to propose that Trx system–orchestrated cellular preemptive Cys persulfidation may provide protection to redox-active enzymes under elevated oxidative stress conditions and thereby preserve key biological functions of the cell. We demonstrated that oxidation of persulfides is prevalent in cells and in vivo and that they can be reduced back by the Trx system to provide the corresponding active Cys thiol forms. This dynamic model represents an important layer of control for protein functions with particular relevance to redox-related biological events (29). Of note, in a parallel study, a similar thiol-protecting model was proposed to play a role in aging-induced oxidative processes (32).

Although sulfur metabolism is becoming increasingly recognized as critical in cancer biology, clinical evidence to support the oncogenic functions of transsulfuration enzymes and data on their contributions to tumor progression remain scarce. In this study, we report that transsulfuration is rewired in BLBC with diverse roles in tumor progression, which are linked to altered Cys persulfidation.

Results

CBS Is Expressed at High Levels in BLBC. To obtain a view of oxidative stress and redox regulation in breast cancer, we used in-depth quantitative proteomics (33) data on 45 breast cancer tumors from the Oslo2 study cohort (34). The 45 tumors were selected to have nine tumors from each PAM50 subtypes. The transsulfuration enzyme CBS stood out by showing markedly elevated protein levels in basal-like tumors compared to the luminal, HER2-negative, and "normal-like" subtypes (Fig. 1*A*, arrow). CBS protein levels are significantly higher in basal-like tumors compared to the other PAM50 subgroups (Fig. 1*B*). This specificity among subtypes suggests that high CBS levels may be related to tumor-driving biology specific to BLBC. The correlation of CBS protein levels to all other proteins [10,090 proteins were measured (34)] displayed enrichment of proliferation-related gene sets in the positively correlating proteins and estrogen response–related genes within the negatively correlating proteins (*SI Appendix*, Fig. S1*A*). Exploiting the data measured on transcriptome and proteome levels on same tumors, we found high correlation between CBS protein and messenger RNA (mRNA) levels (*SI Appendix*, Fig. S1*B*), while neither displayed any correlation to copy number aberrations (*SI Appendix*, Fig. S1*C*). This allowed us to carry out further analyses in different patient cohorts on the mRNA level to corroborate this observation. Breast tumors from Oslo 2 ($n = 372$) (35, 36), TCGA (The Cancer Genome Atlas) ($n = 832$) (37), and NeoAva ($n = 131$) (38) cohorts (*SI Appendix*, Fig. S1 *D–F*) again showed high levels of CBS in BLBC compared to the other PAM50 subtypes.

In order to study treatment response–related behavior, we looked at CBS expression levels in samples from the NeoAva trial; patients with complete response showed significantly elevated CBS levels compared to noncomplete responders (Fig. 1*C*). CBS levels in complete responders (Fig. 1*D*) dropped down significantly by 12 wk and remained there 25 wk after treatment. This was also seen in noncomplete responders but to a lesser extent (*SI Appendix*, Fig. S1*G*), which raises the possibility that CBS could potentially be used as a biomarker of treatment response.

CBS Silencing in BLBC Cells Inhibits Tumor Progression. Quantitative proteomics and Western blot analysis on breast cancer cell lines showed that CBS levels were also highly elevated in a subset of BLBC cells compared to luminal cancer cell subtypes (*SI Appendix*, Fig. S2 *A* and *B*). In order to study the biological roles of up-regulated CBS levels in BLBC, we used short hairpin RNA (shRNA) technology to silence CBS expression in two BLBC cell lines (Cal51 and HCC1143). CBS knockdown was confirmed on the protein level by Western blot analyses (*SI Appendix*, Fig. S2*C*) as well as by CBS activity measurements in lysates using a mass spectrometry–based method (Fig. 2*A*). Cal51 shCBS cells proliferated slower compared to corresponding controls (Fig. 2*B*). In addition, soft agar colony formation assay revealed diminished malignant transformation in shCBS compared to control HCC1143 cells (Fig. 2*C*). To assess how CBS silencing affects tumor growth in vivo, we generated xenograft models with subcutaneous injection of our model BLBC cells into immune-deficient mice. Significantly slower tumor progressions were observed in shCBS compared to control Cal51 and HCC1143 xenografts. Control tumors were visibly

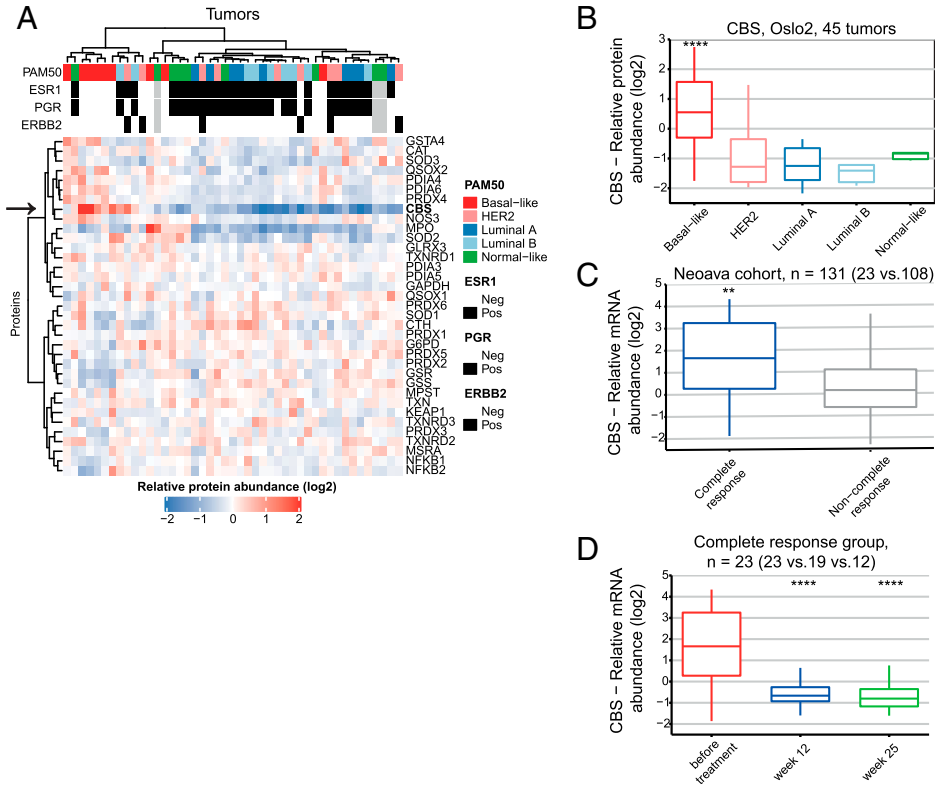

Fig. 1. CBS is expressed at high levels in BLBC. (*A*) Clustering of redox proteins using high-resolution isoelectric focusing quantitative proteomics analysis of 45 breast cancer samples from the Oslo2 cohort. Arrow indicates the protein abundance levels of CBS. Pearson correlation, Ward D2 was used for clustering. (*B*) Boxplot of CBS protein levels in PAM50 subgroups. Quantitation based on in-depth proteomics data, and statistical analysis was performed using DEqMS (basal-like group compared to the rest of the samples). (*C*) CBS mRNA expression levels in treatment-naïve breast tumors subsequently showing complete response versus noncomplete response to treatment in the NeoAva cohort (both treatment arms combined). (*D*) Changes in CBS mRNA expression levels in response to 12 and 25 wk of treatment in complete responders (both treatment arms combined). $^{**}P < 0.01$ and $^{****}P < 0.0001$. In *D*, time points are compared to levels before treatment.

more vascularized compared to shCBS tumors (Fig. 2*D* and *SI Appendix*, Fig. S2*D*).

CBS Plays an Important Role in Proliferation, Angiogenesis, Intratumoral Cancer Cell Necrosis, and the Hypoxic Response of BLBC. To obtain insights into the molecular differences between control and shCBS xenograft tumors, we quantified cancer-related transcripts using the CancerPathway RT^2 Profiler PCR array. Angiogenesis-related genes were altered in both Cal51 and HCC1143 xenografts (*SI Appendix*, Fig. S3). Notably, SERPINF1, an angiogenesis inhibitor, was highly up-regulated in shCBS tumors compared to controls in both tumor types.

Immunohistochemical analyses of Ki67, CD31, and CD34 verified that BLBC cell proliferation and angiogenesis were diminished in HCC1143 and Cal51 shCBS tumors compared to controls (Fig. 3*A* and *SI Appendix*, Fig. S4*A*). Impaired angiogenesis in HCC1143 shCBS xenografts was further confirmed by mRNA analyses of angiogenesis-related gene expressions (Fig. 3*B*). Hematoxylin eosin staining revealed increased intratumoral necrotic areas in CBS-deficient Cal51 and HCC1143 xenografts (Fig. 3*C* and *SI Appendix*, Fig. S4*B*), which could be a direct consequence of inefficient vascularization.

Hypoxia is a key regulator of angiogenesis (39) and tumor cell proliferation as well as necrosis (40). In addition, in BLBC, increased hypoxia-inducible factor (HIF1-α) but not HIF2 levels were found even under normoxic conditions, which was linked to intracellular Cys availability (41). Therefore, the observed differences in angiogenesis, cancer cell proliferation, and necrotic area in the shCBS versus control xenograft tumors could be related to their response to hypoxia. Apart from angiogenesis, a number of hypoxia-related genes were found to be differentially regulated in shCBS versus control tumors (*SI Appendix*, Fig. S3). The hypoxia-related genes are largely regulated by HIF1-α, which is the major transcriptional regulator of hypoxia response in cancer cells. In vitro analyses of hypoxia showed impaired HIF1-α activation in CBS-deficient Cal51 cells. Remarkably, the highly elevated HIF1-α subunit after 6 h of hypoxia in control Cal51 cells was almost undetectable in shCBS Cal51 (Fig. 3*D*). Similarly, CBS silencing decreased HIF1-α levels in HCC1143 cells (*SI Appendix*, Fig. S5*A*). HIF1-α activation was strongly inhibited by pretreatment with the sulfide donor (GYY4137) or with inorganic polysulfides (HS_x^-) in both control and shCBS cells (Fig. 3*D* and *SI Appendix*, Fig. S5*A*).

Elevated Endogenous Oxidative Stress upon CBS Knockdown. Next, we investigated how hypoxia affects gene expression in Cal51 cells in vitro using a Hypoxia Signaling RT^2 Profiler PCR Array. Interestingly, the largest differences in hypoxia-induced gene expressions were observed in glucose metabolic pathways, specifically in 6-phosphofructo-2-kinase/fructose-2,6 bisphosphatase 4 (PFKFB4), which is linked to oxidative stress response (*SI Appendix*, Fig. S5*B*).

The canonical activity of PFKFB4 shunts glucose metabolism back to the pentose phosphate pathway, which is pivotal for cellular protection against oxidative stress. It was recently identified as a potential drug target in prostate cancer because its inhibition caused an impaired balance in ROS production and triggered cancer cell death (42). Despite the diminished hypoxic response, we found that PFKFB4 was elevated in both

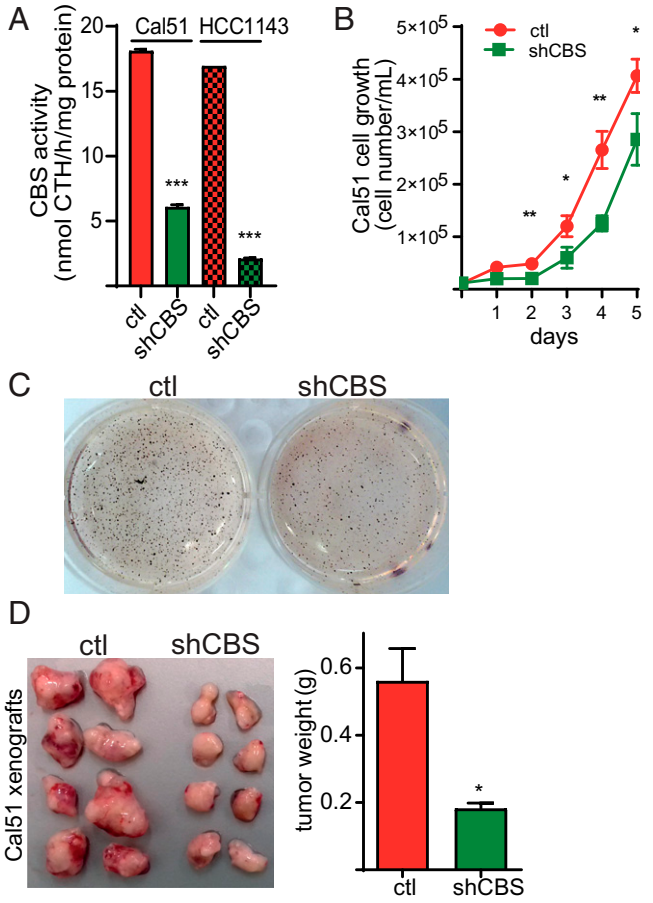

Fig. 2. (*A*) After stable mRNA silencing, CBS activities in Cal51 and HCC1143 control and shCBS cell lysates were measured by a liquid chromatography–tandem mass spectrometry–based method using the EZ:faast kit. The data are means ± SD (n = 3). (*B*) Cal51 cell proliferation in control and shCBS cells were measured daily by cell counting in 6-well plates until they reached full confluency. The data are means ± SD (n = 4). (*C*) Anchorage-independent growth of HCC1143 control and shCBS cells were measured by a soft agar colony assay. Colonies were visualized with nitroblue tetrazolium sodium salt solution staining after 35 d. Picture of wells are representative of three independent samples. (*D*) Cal51 control and shCBS cells were injected into SCID female mice subcutaneously. Xenograft tumors were removed when control tissue volumes reached ∼100 mm^3. After dissection, xenograft tissues were weighted and photographed. The data are means ± SD (n = 8). *P < 0.05, **P < 0.01, and ***P < 0.001 show significant differences in shCBS compared to control samples in each relevant panel. Experiments were repeated at least three times, and representative images are shown.

Cal51 and HCC1143 shCBS xenograft tumors (*SI Appendix*, Fig. S5*C*), potentially related to adaptation to an increased intracellular oxidative stress, which may be more pronounced in CBS-deficient tumor cells.

The pentose phosphate pathway provides the increased NADPH needed for thioredoxin reductase (TrxR) and glutathione reductase, the master regulators of the cell's reducing machinery (43). The need for an increased NADPH supply in BLBC is further corroborated by significantly elevated mRNA levels of TrxR1 (TXNRD1, *SI Appendix*, Fig. S6*A*) and Trx1 (TXN, *SI Appendix*, Fig. S6*B*) in BLBC tumor samples from the NeoAva trial as compared to other PAM50 subtypes. TrxR1 and Trx1 levels were elevated in responders compared to the noncomplete response group (*SI Appendix*, Fig. S6 *C* and *D*) and dropped down significantly during treatment (*SI Appendix*, Fig. S6 *E* and *F*). These observations suggested an increased reducing capacity, which may be related to elevated ROS production in BLBC cells and a role for CBS in the protection against endogenous oxidative stress.

CBS Protects BLBC Tumors from Oxidative Stress and Ferroptotic Cell Death. To investigate whether CBS protects against ROS production, shCBS and control Cal51 and HCC1143 cells were treated with increasing amounts of H_2O_2. H_2O_2-induced exogenous oxidative stress was significantly less tolerated by shCBS cells (Fig. 4*A* and *SI Appendix*, Fig. S7) compared to control cells.

Cys catabolism is tightly regulated by the cysteine dioxygenase (CDO) catabolic pathway (*SI Appendix*, Fig. S8) (16). Lower expressions of key enzymes in this pathway, namely sulfite oxidase (SO) and cysteine sulfinic acid decarboxylase (CSAD) in BLBC, compared to the other PAM50 subtypes of breast tumors indicate a high CySSCy demand of human BLBC tumors (Fig. 4*B*). Furthermore, CySSCy deprivation was reported to induce BLBC necrotic cell death (15). A recent study obtained evidence on SHSY5Y neuroblastoma, LN229 glioblastoma, and SKMEL30 skin cancer cell lines (6) and showed that shCBS cells were significantly more susceptible to CySSCy deprivation than controls. We found that CBS knockdown also sensitized Cal51 cells to CySSCy deprivation–induced cell death (Fig. 4*C* and *SI Appendix*, Fig. S9*A*). In contrast to the observations of Tang et al. (15), CySSCy deprivation–induced Cal51 cell death in our hands was not associated with activation of the MEKK4-p38-NOXA pathway (*SI Appendix*, Fig. S9*B*). On the other hand, ferrostatin potently inhibited Cal51 cell death in CySSCy-deprived medium, suggesting that the lack of adequate CySSCy supply, instead, caused ferroptosis in BLBC cells (Fig. 4*D* and *SI Appendix*, Fig. S9*C*), which agrees with reported observations of Stockwell et al. (44). In addition, CySSCy deprivation–induced lipid peroxidation was elevated in shCBS (Fig. 4*E* and *SI Appendix*, Fig. S9*D*) cells, which is a biomarker of ferroptotic cell death. Moreover, when the cells were grown in reduced CySSCy-containing medium, shCBS cells exhibited more prominent vulnerability to H_2O_2 stress (Fig. 4*F*). In light of these observations and the fact that tumor interstitial fluids provide a CySSCy-depleted environment for the tumor (17), we hypothesize that the observed expanded intratumoral necrotic areas in shCBS BLBC xenograft tumors compared to controls (Fig. 3*C* and *SI Appendix*, Fig. S4*B*) might be due to ferroptotic cell death in the shCBS tumors.

Collectively, these results indicate that the observed elevated CBS levels in BLBC could be related to the CySSCy-addicted phenotype of these tumors, which might not be surprising considering that cells rely on transsulfuration to maintain their Cys need for protection against oxidative stress when the exogenous supply via xCT is diminished.

CBS-Dependent Protein-Cys Persulfidation Contributes to Protection against Oxidative Stress in BLBC Cells. Because CBS is a key enzyme of the transsulfuration pathway, a plausible explanation for an increased vulnerability of shCBS BLBC cells to CySSCy deprivation could be that the cells under these conditions rely on de novo Cys synthesis for GSH production, and hence, canonical transsulfuration becomes pivotal in cellular protection against ROS-induced ferroptotic cell death (6). Based on this and the fact that CBS uses serine (Ser) and HCys in its canonical enzymatic activity to make the Cys precursor cystathionine (*SI Appendix*, Fig. S8), we predicted that CySSCy-deprived conditions would make shCBS cells sensitive to Ser starvation. By contrast, however, elimination of Ser from the growth medium instead had a protective effect on Cal51 shCBS cells under CySSCy-deprived conditions (Fig. 5*A*). This

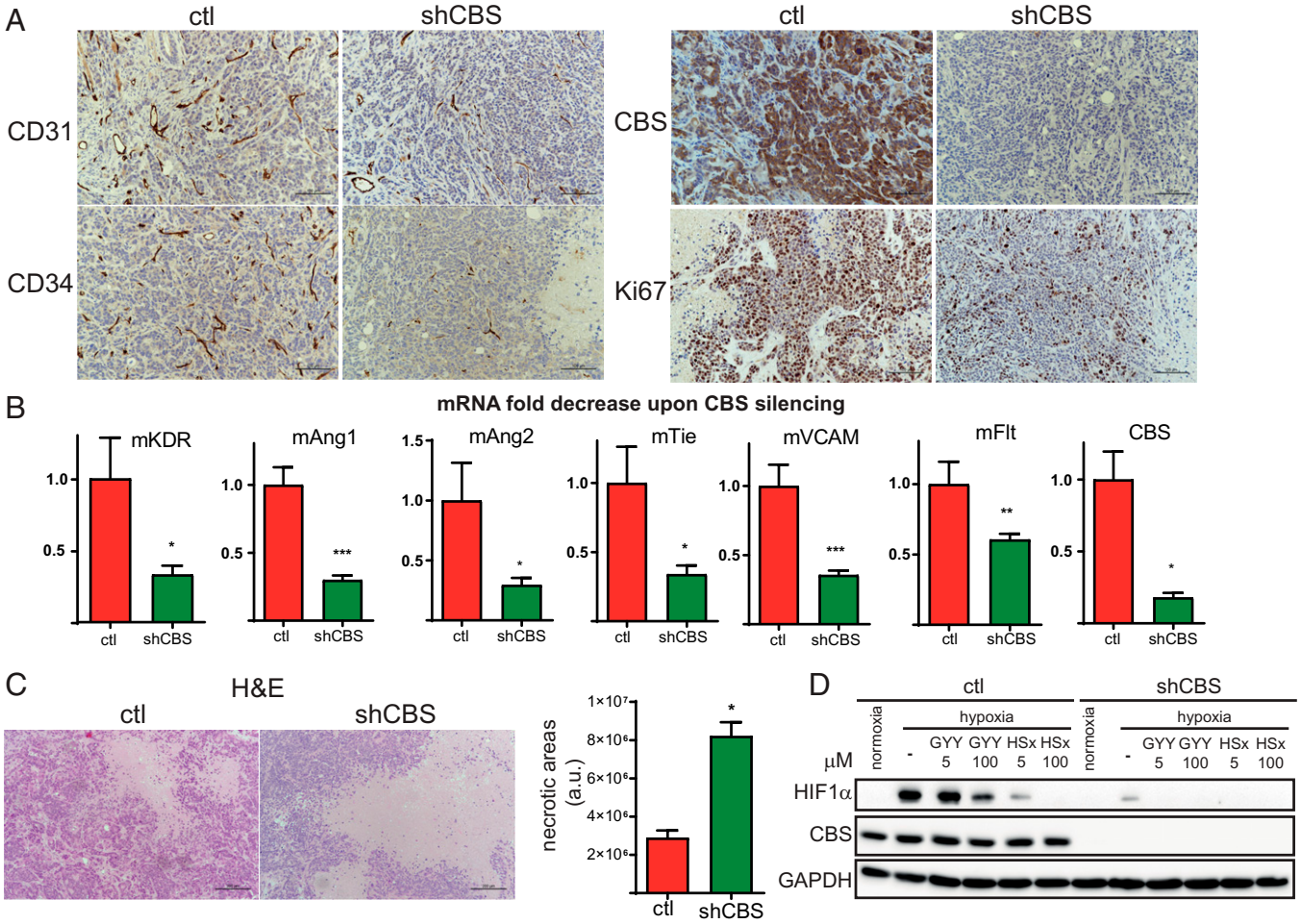

Fig. 3. CBS plays an important role in cell proliferation, angiogenesis, intratumoral cancer cell necrosis, and the hypoxic response in BLBC. (*A*) Immunohistochemistry of HCC1143 control and shCBS xenograft tissues. Proliferation of tumor cells were examined with Ki67 nuclear antigen staining. The formation of intratumoral blood vessels was visualized using CD31 and CD34 markers. CBS protein presence and silencing were confirmed by CBS staining. (*B*) Impaired angiogenesis in shCBS HCC1143 xenograft tumors were further confirmed at the mRNA level by RT-qPCR; kinase insert domain protein receptor (KDR), angiopoetin (Ang) 1 and 2, tyrosine kinase with immunoglobulin-like and EGF-like domains 1 (Tie), FMS-like tyrosine kinase 1 (Flt), vascular cell adhesion molecule 1 (VCAM), and CBS mRNA changes were compared to controls and normalized to actin. (*C*) Histological assessment of intratumoral necrosis in control and shCBS HCC1143 xenografts. (Scale bars: 200 μm.) Necrotic areas were evaluated by the ImageJ software. Representative images are shown. (*D*) In vitro analyses of HIF1-α–mediated hypoxia response in control and shCBS Cal51 cells. Cells were pretreated with 5 and 100 μM sulfide donor GYY4137 (GYY) for 90 min or with 5 and 100 μM polysulfide (HS_x^-) for 30 min where indicated. After 6 h of hypoxia or normoxia, cells were collected, and HIF1-α activations were assessed by Western blot analysis. Experiments were repeated three times, and representative images are shown. $*P < 0.05$, $**P < 0.01$, and $***P < 0.001$ show significant differences in shCBS compared to control samples in *B* and *C*.

suggested that the noncanonical activities of CBS might be more important in this phenotype.

Also suggesting an important role for noncanonical CBS activities, under similar CySSCy deprivation conditions (48 h, 4 μM CySSCy), mass spectrometry–based quantitative sulfur species analyses showed no difference in Cys levels incorporated into proteins (protein-Cys) and a slight increase in GSH levels in shCBS versus control Cal51 cells (Fig. 5*B*). Under similar conditions in HCC1143 cells, CBS silencing also slightly but significantly increased GSH concentrations (*SI Appendix*, Fig. S10*A*). These observations do not support a decreased GSH availability due to impaired Cys supply in shCBS cells under these conditions. Rather, the data suggest that the GSH synthesis machinery in BLBC cells work with increased efficiency in the shCBS cells to be able to compensate for the diminished Cys availability. This hypothesis was corroborated by the observed increased vulnerability of shCBS cells to buthionine sulfoximine (BSO), an inhibitor of GSH synthesis (Fig. 5*C*), and the significantly elevated levels of gamma-glutamylcysteine synthetase (GCLM, the regulatory subunit of the rate-limiting enzyme of GSH biosynthesis) in human basal-like breast tumors (Fig. 5*D*).

The above observations collectively suggest that the vulnerability of shCBS cells to oxidative stress and ferroptotic cell death, compared to control BLBC, is not due to impaired GSH bioavailability but rather linked to Cys utilization via additional pathways. We recently reported that persulfidation provides protection to key protein-Cys residues via oxidizing to perthiosulfinic ($P\text{-}S\text{-}SO_2H$) and perthiosulfonic acid ($P\text{-}S\text{-}SO_3H$) derivatives under oxidative stress conditions. These oxidized perthiol forms, in contrast to the equivalently oxidized thiol forms, sulfinic ($P\text{-}SO_2H$), and sulfonic acids ($P\text{-}SO_3H$), can be readily reduced to thiols by the Trx or GSH systems after the oxidative stress subsides (29). This mechanism is prevalent in cultured cells and in mouse tissues, and it is likely to be an important element of the cells' antioxidant stratagem (29). Importantly, under CySSCy-deprived conditions, we here found lower protein-Cys persulfide and GSH persulfide levels in Cal51 shCBS cells and lower Cys persulfide, sulfide, and thiosulfate (the oxidized form of sulfide)

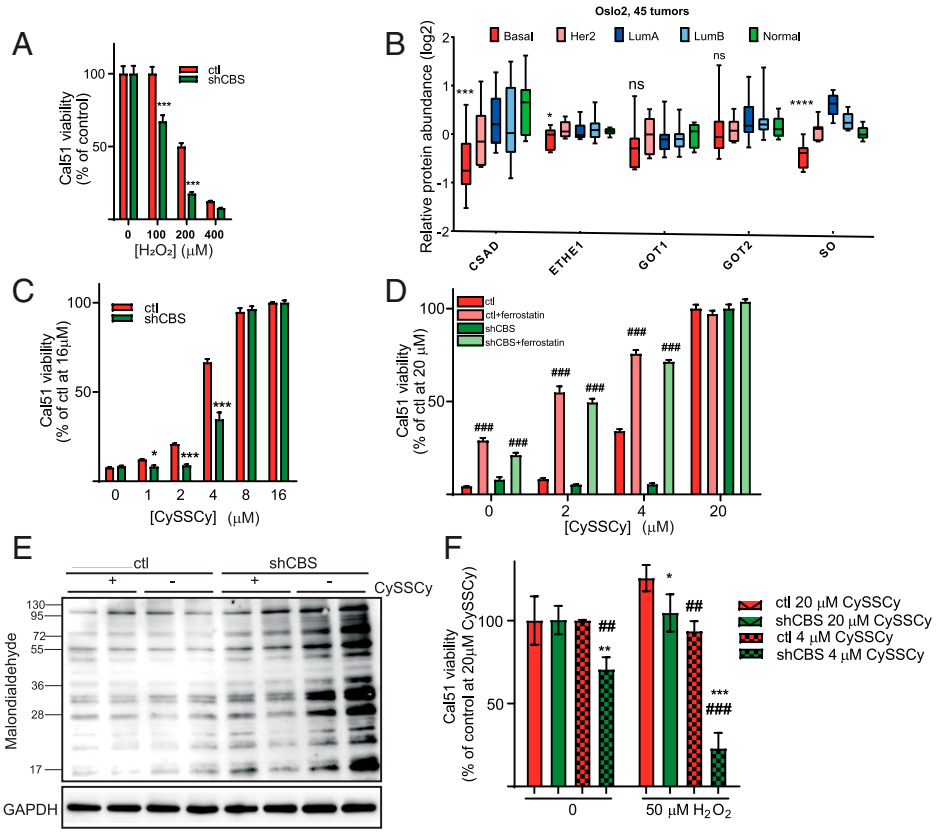

Fig. 4. CBS protects BLBC tumors from oxidative stress and ferroptotic cell death. (*A*) Cellular viability of control and shCBS Cal51 cells as measured with the CCK8 method in which cells were treated with increasing concentrations of hydrogen peroxide for 24 h. Viability was evaluated in percentages by considering nontreated control samples as 100%. $***P < 0.001$ show significant differences in shCBS compared to control samples. Data are means ± SD ($n = 6$). (*B*) Protein levels of transsulfuration enzymes in 45 breast tumors of the Oslo 2 proteomics cohort. For each enzyme, basal subtypes are compared to all other subtypes using DEqMS. ns: $P \geq 0.05$, $****P < 0.0001$. (*C*) Viability of control and shCBS Cal51 cells as measured by the Sulforhodamine B (SRB) method in which cells were maintained in increasing concentrations (0 to 16 μM) of CySSCy for 72 h. Control cells at 16 μM CySSCy were considered as 100% of survival. $*P < 0.05$, $**P < 0.01$, and $***P < 0.001$ show significant differences in shCBS compared to control. The data are means ± SD ($n = 4$). (*D*) Cellular viability was measured with the SRB method for control and shCBS Cal51 cells, which were maintained in increasing concentrations (0 to 20 μM) of CySSCy in the presence or absence of 1 μM ferrostatin for 72 h. $^{###}P < 0.001$ show significant differences between nontreated and ferrostatin-treated control or shCBS cells. The data are means ± SD ($n = 4$). (*E*) Cal51 control and shCBS cells were maintained in normal and CySSCy-free media for 48 h. Western blot analyses were performed using a lipid peroxide marker anti-malondialdehyde antibody. Image is representative of two biological replicates. (*F*) Control and shCBS Cal51 cells were conditioned in 4 and 20 μM CySSCy for 24 h followed by 0 or 50 μM hydrogen peroxide treatment for 24 h. Viability was measured by the CCK8 method. Survival in nontreated cells with 20 μM CySSCy were set as 100%. $*P < 0.05$, $**P < 0.01$, and $***P < 0.001$ show significant differences in shCBS compared to control cells. $^{##}P < 0.01$ and $^{###}P < 0.001$ show significant differences between cells which were maintained in 20 μM and 4 μM CySSCy. The data are means ± SD ($n = 6$). Experiments were repeated three times, and representative images are shown.

levels in HCC1143 shCBS cells compared to the corresponding controls (Fig. 5*E* and *SI Appendix*, Fig. S10*A*).

In parallel with the lower levels of Cys perthiol forms found in the shCBS BLBC cells in culture, GSH persulfide and protein persulfide levels were both significantly diminished in shCBS Cal51 xenografts as compared to control Cal51 tumors (Fig. 5*F*), yet free Cys, HCys, and protein-Cys levels were unaffected (*SI Appendix*, Fig. S10 *B* and *C*). Apart from cystathionine (CTH) synthesis from HCys and Ser, CBS can utilize 1) 2 Cys to make sulfide, also yielding lanthionine (LTH) as a secondary product (45), or 2) CySSCy to produce Cys persulfide (Fig. 5*G*) (24). Hence, the lower free Cys, CySSCy, together with the lower cystathionine and lanthionine (LTH) levels (*SI Appendix*, Fig. S10*D*) suggest an impaired activity of these CBS-dependent enzyme functions and diminished production of sulfide and Cys persulfide in shCBS as compared to control tumors. Based on these observations, we propose that elevated CBS levels might contribute to cellular protection against oxidative stress in BLBC tumors via promoting protein-Cys persulfidation. As depicted on Fig. 5*G*, this can occur alternatively via 1) supplying Cys for CARS2 (which is also significantly elevated in human BLBC as compared to the other PAM50 subtypes) (Fig. 5*H*) to make Cys persulfide, 2) supplying Cys for CSE to make sulfide, 3) using Cys as a CBS substrate to make sulfide, or 4) using CySSCy as substrate to directly produce Cys persulfide (*Discussion*). Sulfide and Cys persulfide species subsequently can induce protein-Cys persulfidation via oxidative or translational pathways (30, 46), which will protect key protein-Cys residues from irreversible oxidative inactivation (29).

Protein Tyr Phosphorylation Is Impaired in CBS Knockdown Cells and Xenograft Tumors. Besides serving as a protecting group from irreversible oxidative inactivation, we have previously demonstrated that Cys polysulfidation and its redox reactions inhibit key phosphatase activities, including PTEN (23) and protein tyrosine phosphatase 1B (PTP1B) (29). Inhibited phosphatase persulfides and their oxidized forms are reduced back to their active thiol forms by the Trx1 system, representing a dynamic regulatory mechanism. In squamous carcinoma cells, we demonstrated that EGF-induced Tyr phosphorylation is increased by polysulfide treatment–induced protein persulfidation, which was potentiated by lack of selenium supplementation (needed for

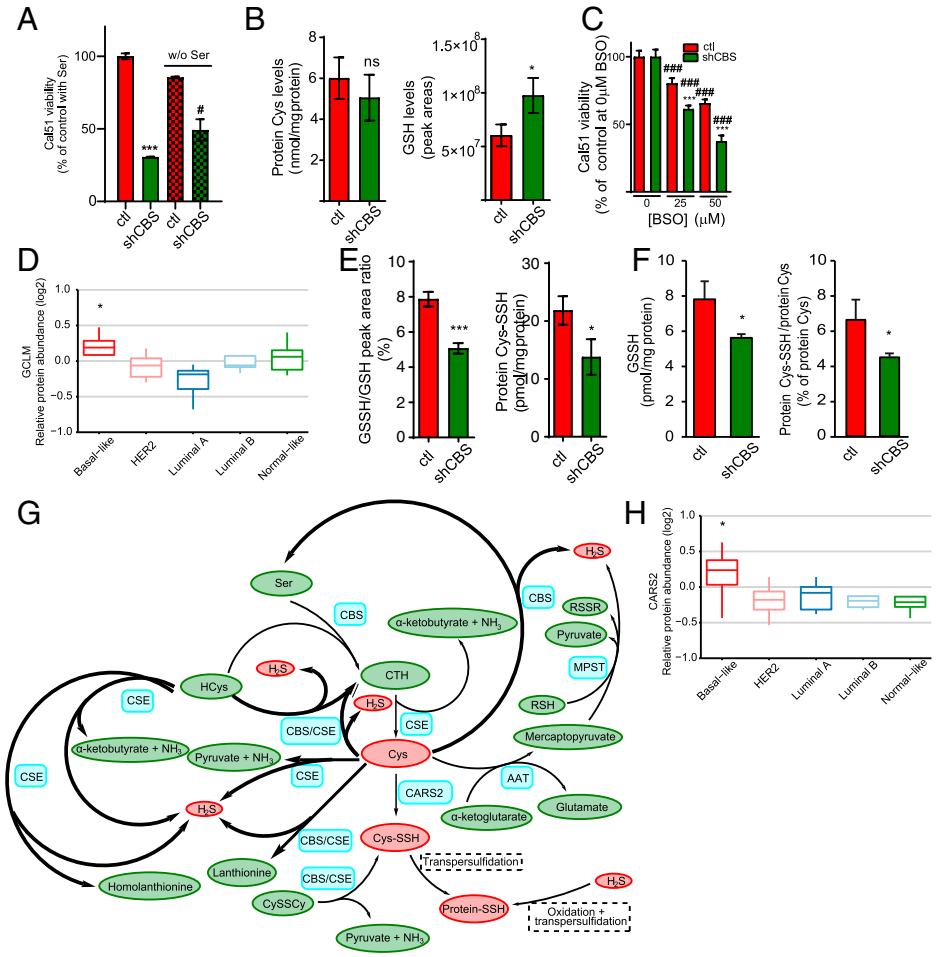

Fig. 5. CBS-dependent protein-Cys persulfidation contributes to protection against oxidative stress in BLBC cells. (*A*) Viability of control and shCBS Cal51 cells as measured by the Sulforhodamine B (SRB) method in which cells were maintained in 4 μM CySSCy in the presence or absence of 250 μM serine for 72 h. Results are presented in percentage in which the viability of control cells in 250 μM serine were set as 100%. ***$P < 0.001$ shows significant differences in viability of shCBS compared to control cells. $^{\#}P < 0.05$ shows significant differences between serine-deprived and nondeprived conditions. The data are means ± SD ($n = 6$). (*B*) Levels of protein incorporated Cys content and intracellular GSH in control and shCBS Cal51 cells in which cells were maintained in 4 μM CySSCy for 48 h followed by β-(4-hydroxyphenyl)ethyl iodoacetamide (HPE-IAM) labeling and liquid chromatography–tandem mass spectrometry (HPLC-MS/MS) analyses. The data are means ± SD ($n = 3$). ns: $P \geq 0.05$ and *$P < 0.05$ shows a significant difference in control compared to shCBS cells. (*C*) Cellular viability measured by the SRB method in Cal51 control and shCBS cells in which cells were treated with increasing concentrations of the GCLM inhibitor BSO for 72 h. Viabilities of nontreated cells were set as 100%. $^{\#\#\#}P < 0.001$ shows significant differences in BSO-treated compared to the corresponding nontreated samples. ***$P < 0.001$ shows significant differences in shCBS compared to control cells. The data are means ± SD ($n = 6$). (*D*) Protein levels of human GCLM in different PAM50 subtypes of 45 breast tumors from the Oslo 2 cohort. Basal subtype is compared to all other subtypes, *$P < 0.05$. (*E*) Levels of protein and GSH Cys persulfidation were analyzed using HPLC-MS/MS in Cal51 control and shCBS cells, which were cultured in 4 μM CySSCy for 48 h and labeled with HPE-IAM. GSSH/GSH represents the percentage of GSH persulfide to GSH calculated from peak areas (*Left*). Protein-Cys–SSH represents the amount of persulfidated Cys incorporated in the total proteome (*Right*). The data are means ± SD ($n = 3$). *$P < 0.05$, and ***$P < 0.001$ show significant differences in shCBS compared to control cells. (*F*) GSSH (*Left*) and protein-Cys polysulfidation (*Right*) levels in Cal51 control and shCBS tumor xenografts were measured by HPLC-MS/MS. *$P < 0.05$ shows significant differences in shCBS compared to control tumors. The data are means ± SD ($n = 3$). (*G*) Schematic representation of H_2S and persulfide production from endogenous Cys. Blue denotes enzymes, yellow denotes metabolites, red indicates the sulfur containing metabolites that play central roles in persulfidation, and bold arrows indicate the H_2S-producing processes of CBS and CSE. AAT: aspartate aminotransferase, MPST: 3-mercaptopyruvate sulfurtransferase, CTH: Cystathionine, Cys-SSH: Cysteine-persulfide, Protein-SSH: protein with persulfidated Cys, RSH: reduced thiol, RSSR: oxidized thiol, Ser: serine, HCys: homocysteine, CySSCy: cystine. (*H*) CARS2 protein levels in PAM50 subtypes of 45 breast tumors from the Oslo 2 cohort. The basal-like subtype is compared to all other subtypes, *$P < 0.05$. All experiments were repeated at least three times, and representative images are shown.

proper TrxR1 activity) or knockdown of the thioredoxin family enzyme TRP14 (29). Therefore, we here investigated whether CBS knockdown-induced diminished protein persulfidation in BLBC cells could inhibit Tyr phosphorylation processes. Indeed, we observed a reduced overall EGF-triggered Tyr phosphorylation pattern in HCC1143 and Cal51 shCBS cells (*SI Appendix*, Fig. S11 *A* and *B*) as well as in shCBS xenograft tumors (*SI Appendix*, Fig. S11*C*) compared to the corresponding controls. We also investigated differences in EGFR Tyr phosphorylation sites and found that it was significantly lower at Tyr-1068 upon EGF treatment. In addition, phosphorylation of the downstream MEK1/2 was also significantly lower in shCBS HCC1143 cells (*SI Appendix*, Fig. S11*D*). These observations forecast that CBS-related persulfidation events govern Tyr phosphorylation pathways in BLBC tumor cells, which may partially explain the slower proliferation of CBS-silenced cells in cell culture (Fig. 2*B*) and in xenograft tumors (Fig. 3*A* and *SI Appendix*, Fig. S4*A*).

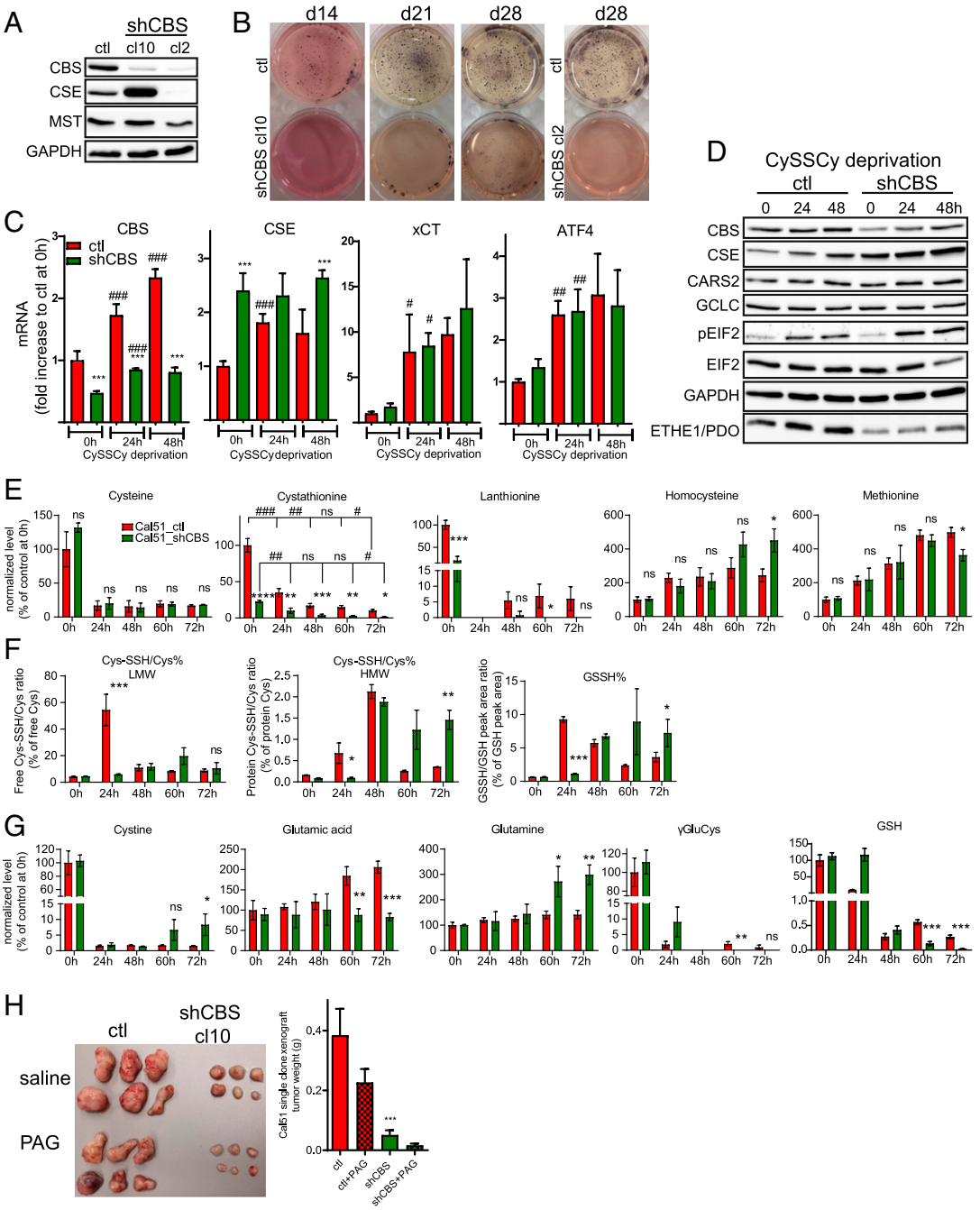

Fig. 6. CSE can compensate to some extent for the effects of CBS knockdown, but targeting both enzymes is lethal for BLBC tumors. (*A*) Expression levels of CBS, CSE, and MPST is shown by Western blot in Cal51 shCBS single-clone cells (cl10 and cl2). (*B*) Anchorage-independent growth of Cal51 control and shCBS single-clone cells were measured by a soft agar colony assay. Colonies were visualized after 14, 21, and 28 d with nitroblue tetrazolium sodium salt solution staining. No colonies were detected in Cal51 shCBS single-clone 2 which failed to overexpress CSE. (*C*) RT-qPCR analysis of CBS, CSE, ATF4, and xCT (SLC7A11) in Cal51 control and shCBS single-clone cells after 0, 24, and 48 h of CySSCy deprivation. Actin, GAPDH, and β2M were used as housekeeping genes. $^{*}P < 0.05$, $^{**}P < 0.01$, and $^{***}P < 0.001$ show significant differences in shCBS compared to control cells. $^{\#}P < 0.05$, $^{\#\#}P < 0.01$, and $^{\#\#\#}P < 0.001$ show significant differences in time points compared to the previous time points in the same cell type. The data are means ± SD ($n = 4$). (*D*) Western blot analyses of CBS, CSE, CARS2, GCLC, eIF2, pEIF2, ETHE1/PDO from control and shCBS single-clone cells after 24 and 48 h of CySSCy deprivation. (*E–G*) Metabolite analyses using the EZ:faast kit (Cys, cystathionine [CTH], HCys, Met, Lanth, CySSCy, Glu, GLN, gGluCys) or the β-(4-hydroxyphenyl)ethyl iodoacetamide (HPE-IAM) labeling based liquid chromatography–tandem mass spectrometry (HPLC/MS-MS) method (Cys-SSH/Cys% HMW, Cys-SSH/Cys% LMW, GSSH%, GSSH LMW) in Cal51 control and shCBS single-clone cells, which were CySSCy deprived for 24, 48, 60, and 72 h. Cys, CTH, HCys, Met, Lanth, CySSCy, Glu, GLN, and gGluCys levels are presented as percentage of the corresponding control samples at t = 0, which were set as 100%; GSSH% represents the percentage of GSH persulfide to GSH, which were calculated from peak areas; Cys-SSH/Cys% LMW and Cys-SSH/Cys% HMW represents the percentage of Cys persulfide to Cys, which were calculated from their respective concentrations in which LMW refers to free and HMW refers to protein-bound cysteines. ns: $P \geq 0.05$, $^{*}P < 0.05$, $^{**}P < 0.01$, $^{***}P < 0.001$, and $^{****}P < 0.0001$ show significant differences in shCBS compared to control samples. $^{\#}P < 0.05$, $^{\#\#}P < 0.01$, $^{\#\#\#}P < 0.001$, and $^{\#\#\#\#}P < 0.0001$ show significant differences in timepoints compared to the previous timepoints in the same cell type. The data are means ± SD ($n = 3$). (*H*) Cal51 control and shCBS single clones were injected in female SCID mice subcutaneously. Mice received PAG or saline at 50 mg per body weight (kg) twice a week. After termination, xenograft tissues were removed, photographed, and weighted. $^{***}P < 0.001$ show significant differences in shCBS compared to control tumors. All experiments were repeated at least three times, and representative images are shown.

CSE Can Compensate to Some Extent for the Effects of CBS Knockdown, but Targeting Both Enzymes Is Lethal for BLBC Tumors. We observed that the diminished CBS activity comes back to almost control levels in shCBS Cal51 cells after 50 passages (*SI Appendix*, Fig. S12). This suggested that silencing efficiency could be varied in the culture of Cal51 cells that may lead to a heterogeneous cell population. Hence, we supposed that cells with higher CBS levels and corresponding higher replication rate overgrow cells that efficiently silenced CBS. Therefore, we produced new shCBS cell lines that were grown from single clones. In most single clones, we observed a significant elevation of CSE, except for the cl2 cell line (Fig. 6*A*). The colony formation ability of single-clone shCBS cells were largely inhibited, which is consistent with a less aggressive phenotype with an extreme case for the cl2 cell line which was not viable at all, indicating that CSE to some extent could compensate for CBS knockdown (Fig. 6*B*). The fact that both CBS's and CSE's transsulfuration activities are needed for endogenous Cys production suggests that the compensatory effect of CSE elevation in single-clone shCBS cells is unlikely to be due to providing backup in cellular Cys supply but rather due to their noncanonical sulfide/persulfide-producing activities, again corroborating that it is the noncanonical CBS activities that are pivotal for BLBC tumor progression. We chose cl10 for further experimentation in order to gain deeper mechanistic insights. When cells were grown under Cys-deprived conditions, expression of CBS, CSE, ATF4, and xCT genes gradually increased over a 48-h time scale (Fig. 6*C*), consistent with these cells having a Cys-addicted phenotype. Because elevated expression of these proteins was accompanied by more prominent phosphorylation of eIF2 (Fig. 6*D*), we suspect that this was likely caused by a stress response–mediated increase in ATF4 levels. Time-resolved transsulfuration metabolome analyses over a 72-h period in fully CySSCy-deprived media showed a decline of cystathionine levels over time in which CTH levels were significantly lower in shCBS compared to the corresponding control cells at every timepoint (Fig. 6*E*). This could be due to increased CSE function, diminished CBS function in shCBS cells, or both since cystathionine is a product of CBS and a substrate for CSE (*SI Appendix*, Fig. S8). However, although the expected time-resolved drop in endogenous Cys concentrations were observed over time in both cell lines, no differences could be detected between shCBS and control cells (Fig. 6*E*). This is consistent with the fact that cellular Cys concentrations are held within tight limits via regulation of both synthesis and turnover of free Cys (16). Impaired Cys consumption by CBS for H_2S production in shCBS cells could contribute to this. Consistent with this notion, impaired LTH synthesis was observed in shCBS cells, which suggests an inhibited flux through the CBS-catalyzed reaction that uses 2 Cys to produce LTH and H_2S (Fig. 6*E*). Despite the large differences in cystathionine concentrations at the early time points, the differences in HCys concentrations only appeared after 60 h (Fig. 6*E*). This was surprising because impaired transsulfuration-induced accumulation of HCys is expected in CBS deficiency (47). The accumulation of HCys due to impaired CBS function could result in an increased flux of remethylation in which HCys is used for Met synthesis; however, no differences were observed in Met levels between shCBS and control cells either (Fig. 6*E*). Therefore, we hypothesize that the excess HCys in shCBS cells is being consumed by the H_2S-producing activities of CSE (Fig. 5*G*), which may become the prominent activity of CSE under conditions when it shows increased expression levels concomitant with decreased cystathionine availability in shCBS cells.

We also observed diminished ratios of Cys persulfide/Cys thiol in both proteins and in low molecular weight metabolites, including GSH persulfide/GSH thiol levels, at 24 h, albeit with a gradual switch in these ratios over time (Fig. 6*F*). Importantly, the redox status of GSH (the GSH/GSSG ratio) and the $NADP^+$/NADPH ratio was similar in the control and shCBS cells (*SI Appendix*, Fig. S13 *A* and *B*). Hence, we propose that at this early 24-h timepoint, the higher basal persulfidation levels are due to rewired transsulfuration activities, which may serve as a front-line protection mechanism of Cys residues from the increasing endogenous oxidative burden. On the other hand, the switch in the persulfidation pattern over time toward more persulfide in shCBS cells compared to controls, together with the increase in CySSCy levels in shCBS cells (Fig. 6*G*), might represent artifactual persulfide and disulfide formation in dying cells due to a catastrophic buildup of ROS. This is in line with the faster ferroptotic cell death of shCBS cells compared to controls in which the differences in viability started to be visible after 48 h, and the majority of the shCBS cells were dead at the 60-h timepoint. This type of ROS-induced intracellular oxidative stress in dying cells was previously demonstrated via the oxidation status of peroxiredoxins (48). In addition, we observed evidence of impaired glutaminolysis (higher intracellular glutamate and lower glutamine) and GSH synthesis (lower γGlu-Cys and GSH levels) at these later timepoints in shCBS cells compared to the controls, which may also be due to oxidation-induced cell death (Fig. 6*G*).

The hypothesis that viable shCBS cells need persulfides for protection against intracellular oxidative stress and other biological processes is further supported by diminished expression of the persulfide-catabolizing persulfide dioxygenase (ETHE1/PDO) enzyme in these cells as compared to controls (Fig. 6*D*; for catabolic pathways, refer to *SI Appendix*, Fig. S8). The fact that ETHE1 levels were significantly lower in BLBC as compared to in other PAM50 subtypes of human breast cancers supports the human in vivo relevance of this observation (Fig. 4*B*).

Finally, to assess the in vivo vulnerability of BLBC tumors to impaired CBS and CSE functions, we produced xenografts from control and shCBS cells cloned from single cells, and following tumor growth, we treated the mice with the specific CSE inhibitor PAG. Similar to the heterogeneous populations, the clonal shCBS tumors grew significantly slower compared to clonal controls (Fig. 6*H*). Importantly, administration of PAG diminished tumor growth in both populations, with the most dramatic impacts on the growth of shCBS tumors. These observations strongly suggest that Cys metabolism is pivotal for BLBC tumor growth, that CSE overexpression can to some extent compensate for CBS disruption in tumor progression, and that the combined targeting of both CBS and CSE could provide a novel efficient strategy for drug development endeavors in BLBC.

Discussion

In this study, we demonstrate that BLBC tumors are unique among the PAM50 subtypes by having a reprogrammed Cys metabolism in order to compensate for their high Cys demand. Proteomics-based expression profile analyses on human BLBC tumors revealed elevated levels of the transsulfuration enzyme CBS and the mitochondrial cysteinyl-tRNA synthetase CARS2. These analyses also revealed significantly diminished expressions of Cys-catabolizing enzymes of the CDO pathway, SO and CSAD. Furthermore, we observed increased expressions of Trx1, TrxR1, and GCLM and demonstrated that rewired Cys metabolism in BLBC cells results in an elevated oxidative stress response. A Cys-addicted phenotype of BLBC cells has recently also been reported by another group (15). That study concluded that Cys is required for GSH synthesis to protect BLBC cells from ROS-induced necrotic cell death via the MEKK4-p38-NOXA pathway. However, in our hands, CySSCy starvation induced ferroptosis rather than necrotic cell death in BLBC cells. Albeit in different cell lines, CySSCy starvation–induced ferroptosis was also reported and linked to glutaminolysis via

the tricarboxylic acid (TCA) cycle (49). Glutamate or its downstream TCA metabolites were shown to be essential to induce mitochondrial hyperpolarization under these conditions, which was proposed to induce elevated oxidative phosphorylation and collateral increases in ROS production, subsequently leading to lipid peroxidation (49). Hence, less activity via the CySSCy/glutamate antiporter xCT was suggested to boil down to elevated mitochondrial oxidative stress.

In the current study, we focused on the roles of the observed elevated CBS levels in BLBC. We here show that CBS protects BLBC cells from oxidative stress and Cys starvation–induced ferroptotic cell death. A major unresolved question in the field is how rewired transulfuration exerts its cancer-protecting functions on a molecular level. Previously, evidence was accumulated that an increased transsulfuration flux via elevated CBS expression levels contributes to more efficient endogenous glutathione production, which plays an important role in cancer cell protection (6). However, beside the canonical activity of CBS to promote Cys synthesis using Ser as a substrate via transsulfuration, noncanonical CBS activity using Cys as a substrate can produce H_2S, a reactive molecule which is a featured small molecule biological mediator with important roles in cancer biology (19). Cancer-promoting functions of H_2S have been reported in colon and lung cancer via stimulation of mitochondrial bioenergetics and angiogenesis or via stimulation of mitochondrial DNA repair (50–52). Elevated CBS levels were recently reported in breast cancer cells, albeit in a nonsubtype-specific manner (53). This latter study suggested a role of the CBS H_2S producing functions in protection against macrophage-induced oxidative stress (53).

Many observed biological functions of H_2S are related to protein-Cys persulfide formation (30). However, a common caveat of most currently available H_2S and persulfide detection methods is that they can hardly discriminate between these sulfur species, which complicates the interpretation of data based on these analyses (54, 55). Furthermore, CBS can also use CySSCy to directly—without the involvement of H_2S—produce free Cys persulfide, which can subsequently induce protein-Cys persulfide formation via transpersulfidation pathways (24). Cys persulfidation can also be induced indirectly by CBS via providing an elevated flux of Cys to CARS2, which functions as a primary Cys persulfide–producing enzyme under normal cell physiological conditions (28). The partitioning of these enzymatic activities in endogenous Cys persulfide production and the roles of H_2S in these pathways has become the subject of many investigations. Currently, a common view in the field and, indeed a perspective that we share, is that these are all viable mechanisms in endogenous situations, and their relative prevalence depends on the biological conditions that cells encounter. Cys persulfidation is both a dynamic activity-regulating protein modification as well as an important mechanism of protecting critical protein thiols against oxidative damage (29, 30). In addition, we recently demonstrated that Cys persulfides interact with the mitochondrial electron transport chain to feed bioenergetics and protect against membrane depolarization (28).

The current study shows that Cys metabolism in BLBC tumors is wired toward elevated Cys production and diminished catabolism and that BLBC tumors have up-regulated antioxidant enzymes on both the Trx1 and GSH pathways. shCBS BLBC xenografts had larger necrotic central regions, and cultured shCBS BLBC cells were more sensitive to CySSCy deprivation–induced ferroptosis, the latter of which was not exacerbated by concomitant serine depletion of the growth medium. Although shCBS cells were more sensitive to oxidative stress, they showed no diminished GSH levels or different GSH/GSSG, $NADP^+$/NADPH status but, rather, had a significant drop in Cys persulfidation. Finally, the loss of CBS could be compensated by CSE up-regulation, and clonal shCBS xenograft tumors were sensitive to the administration of a CSE inhibitor. Together, these observations strongly suggest that the persulfide-producing functions of CBS are important in the Cys-dependent phenotype of BLBC cells and tumors. This is consistent with the fact that the persulfide-catabolizing enzyme ETHE1 was down-regulated in shCBS Cal51 xenografts compared to controls and in human BLBC tumors compared to other PAM50 subtypes. In addition, despite being key enzymes of the CDO pathway, the levels of GOT1 and GOT2 were not significantly lower in basal-like tumors, which may be due to the fact that they also play important roles in persulfide production as we demonstrated in our recent publication (56), most likely via contribution to H_2S production along with MPST (*SI Appendix*, Fig. S8).

In the current study, disruption of CBS inhibited both the BLBC hypoxic response and tumor angiogenesis. A previous study suggested that triple-negative breast cancers inhibit CySSCy flux through xCT via excreting large amounts of glutamate, since xCT is a CySSCy glutamate antiporter. This, in turn, was proposed to result in HIF1-α activation via diminished Cys-mediated protection of hypoxia-inducible factor prolyl hydroxylase 2 (HIF-PH2) from oxidative stress, thereby stabilizing HIF1-α to promote the hypoxic response of breast cancer cells (41). However, this model is not consistent with the Cys-addicted phenotype of these cells observed herein and reported in other studies (6, 15). Taking these observations into account, we propose that the elevated levels of CBS in BLBC could, instead, drive HIF-PH2 inactivation via persulfidation of specific Cys residues. Notwithstanding, in stark contrast to this hypothesis and our observation that CBS knockdown strongly abrogated the HIF1-α response to hypoxia, a recent study on HUVEC and HAoEC endothelial cells found that CBS inhibition stabilized HIF1-α via protecting HIF-PH2 through persulfidation of specific zinc finger domain Cys residues (57). The authors suggested that exogenous administration of H_2S or GYY4137 (a common H_2S donor compound) could rescue CBS inhibition–induced HIF1-α stabilization. Consistent with the latter observation in our systems, we also found that administration of GYY4137 or inorganic polysulfides efficiently inhibited the HIF1-α signal under hypoxic conditions (Fig. 3*D* and *SI Appendix*, Fig. S5*A*). The apparently contradicting observations might be due to differences in the compartment-specific partitioning of canonical and noncanonical CBS activities in different cellular systems and under disease versus normal conditions. Future detailed mechanistic studies will be needed to gain deeper insights into the underlying reasons of these apparently discordant observations.

Apart from protecting BLBC cells from exogenous and endogenous oxidative stress, we have shown that persulfidation is an important mediator of Tyr phosphorylation cascades via orchestrating the activities of phosphatase enzymes (29). Thus, CBS silencing inhibits Tyr phosphorylation in BLBC cells and xenograft tumors, which could also contribute to the observed inhibited cell proliferation and tumor progression of shCBS cells and xenografts. Based on the reported roles of persulfidation in mediating PTP1B and PTEN activities (23, 29, 30, 58), we believe that CBS silencing-induced impaired persulfidation of phosphatase Cys residues is likely to be the mechanism underlying the observed loss in Tyr phosphorylation; however, a systematic study investigating the specific roles of persulfidation on different members of the kinase and the phosphatase family of enzymes in these conditions is in order.

Finally, we report that overexpression of CSE can compensate for CBS silencing and that CSE inhibition in shCBS xenografts was extremely effective in inhibiting Cal51 tumor growth.

On clinical grounds, our discoveries set the stage for novel targeted drug development endeavors in BLBC by building on the observations that these tumors are highly addicted to Cys and that their transsulfuration machinery is rewired for more

Cys production and utilization. These, together with the fact that the tumors' microenvironment is Cys deprived compared to the normal tissues', predict that targeting CBS and/or CSE in BLBC could potentially provide a clinical benefit for patients, which could address a critical need in medical oncology. Moreover, the efficiency of therapy can be monitored by assessing the enzyme levels of the aforementioned transsulfuration pathways, giving rise to new diagnostic opportunities to follow treatment progression and patient response based on our findings.

Materials and Methods

Lentiviral Transduction. For shRNA-mediated stable knockdown, we used the MISSION Lentiviral-Mediated Gene-Specific shRNA system (Sigma). For CBS knockdown, we used MISSION shRNA Lentiviral Transduction Particles (SHCLNV-NM_000071, ID: TRCN0000291407). Its corresponding control was MISSION pLKO.1-puro empty vector control transduction particle (#SHC001V). There are more details in *SI Appendix, Supporting Materials and Methods*.

Soft Agar Colony Assay. Colony formation was performed as described in ref. 59. There are more details in *SI Appendix, Supporting Materials and Methods*.

CySSCy Deprivation. Deprivation medium was prepared according to ref. 15 with slight modifications. There are more details in *SI Appendix, Supporting Materials and Methods*.

Cellular Viability. Cellular viability was measured by Sulforhodamine B assay and by using a Cell Counting Kit-CCK8 (Dojindo). There are more details in *SI Appendix, Supporting Materials and Methods*.

Xenografts. All animal model protocols were carried out in accordance with the Guidelines for Animal Experiments and were approved by the Institutional Ethics Committee at the National Institute of Oncology, Budapest, Hungary (permission no.: PEI/001/2574–6/2015). Female severe combined immunodeficiency (SCID) mice (CB17/Icr-Prkdcscid) for Cal51 and female NODSCID mice (NOD.Cg-Prkdcscid) for HCC1143 from our colony were used for the experiments. There are more details in *SI Appendix, Supporting Materials and Methods*.

CBS Activity and Metabolite Measurements. For metabolomics analyses, lysates were derivatized and measured with the EZ:Faast Kit (Phenomenex) using a Thermo Vanquish UHPLC system coupled to a Thermo Q Exactive Focus mass spectrometer. For CBS activity measurements, lysates were prepared as published previously (60). There are more details in *SI Appendix, Supporting Materials and Methods*.

Liquid Chromatography–Tandem Mass Spectrometry Measurements of Low and High Molecular Weight Persulfides/Polysulfides. Measurements were based on the method published by Akaike et al. (28) and performed in Hungary or in Japan as described in *SI Appendix, Supporting Materials and Methods*.

Data Analyses. Plotting and statistical analyses were performed using GraphPad Prism 5.03 (GraphPad Software, Inc.) or R (R Core Team). Plotted values show the means, and the corresponding error bars represent the SDs of at least $n = 3$ replicates. Measured values were compared using Student's t test except for the proteomics data (Figs. 1*B*, 4*B*, and 5 *D* and *H*) in which differential expression analysis of quantitative mass spectrometry (DEqMS) was used (61). Significances on Figs. 1*B*, 4*B*, and 5 *D* and *H* and *SI Appendix*, Fig. S1 *D–F* represent significant differences between basal and all other groups.

Relevant significances are explained in the figure legends and denoted on the graphs depending on the obtained P values in the following way: $^{*}P < 0.05$, $^{**}P < 0.01$, $^{***}P < 0.001$, and $^{****}P < 0.0001$ show significant differences in shCBS compared to control. $^{\#}P < 0.05$, $^{\#\#}P < 0.01$, $^{\#\#\#}P < 0.001$, and $^{\#\#\#\#}P < 0.0001$ show significant differences in treatment or between time points compared to the corresponding nontreated samples or previous time points in the same cell type, respectively.

Bioinformatics Analyses of Redox and Antioxidant Genes in Breast Tumor Cohort and Cell Lines. Protein and mRNA data for breast tumors and cell lines were from previously published papers and presented as the binary logarithm of their ratio compared to the means of the whole dataset. Quantitative mass spectrometry–based proteomics data of 45 breast tumors were from ref. 34. TCGA RNA data for 832 breast tumors were from ref. 37, and 17 breast cell lines were from Zhu et al. (61). All analyses were performed in R using the following packages: ggpubr, ggExtra, ComplexHeatmap, circlize, corrr, hyper, DEqMS, and patchwork.

Data Availability. All study data are included in the article and/or *SI Appendix*.

ACKNOWLEDGMENTS. This work was supported by the 2019 Hungarian Thematic Excellence Program TUDFO/51757/2019-ITM, TKP2020-NKA-26, the National Laboratories Excellence Program (under the National Tumorbiology Laboratory Project), and KH_126766, K_129286 from the Hungarian National Research, Development and Innovation Office. P.N. acknowledges the Japan Society for the Promotion of Science (Invitational Fellowship L19520). M.K., O.C., and P.N. acknowledge financial support from the NVKP_16-1-2016-0005 from the Hungarian National Research, Development and Innovation Office. J.L. is supported by financing from the European Union's Horizon 2020 Research and Innovation Programme for the RESCUER project under Grant Agreement No. 847912, the Swedish Research Council, the Swedish Cancer Society, the Swedish Foundation for Strategic Research, and the Stockholm County Council; J.L. and H.J.J. are supported by the Cancer Society in Stockholm. The excellent technical assistance by Anna Mária Tóth and Anita Hidvégi and the valuable intellectual input and proofreading of the manuscript by Ed Schmidt are greatly appreciated.

1. C. M. Perou *et al.*, Molecular portraits of human breast tumours. *Nature* **406**, 747–752 (2000).
2. R. A. Cairns, I. S. Harris, T. W. Mak, Regulation of cancer cell metabolism. *Nat. Rev. Cancer* **11**, 85–95 (2011).
3. R. J. DeBerardinis, N. S. Chandel, Fundamentals of cancer metabolism. *Sci. Adv.* **2**, e1600200 (2016).
4. A. Schulze, A. L. Harris, How cancer metabolism is tuned for proliferation and vulnerable to disruption. *Nature* **491**, 364–373 (2012).
5. R. Weber, K. Birsoy, The transsulfuration pathway makes, the tumor takes. *Cell Metab.* **30**, 845–846 (2019).
6. J. Zhu *et al.*, Transsulfuration activity can support cell growth upon extracellular cysteine limitation. *Cell Metab.* **30**, 865–876.e5 (2019).
7. T. Finkel, Signal transduction by reactive oxygen species. *J. Cell Biol.* **194**, 7–15 (2011).
8. P. Nagy, Kinetics and mechanisms of thiol-disulfide exchange covering direct substitution and thiol oxidation-mediated pathways. *Antioxid. Redox Signal.* **18**, 1623–1641 (2013).
9. S. G. Rhee, Cell signaling. H2O2, a necessary evil for cell signaling. *Science* **312**, 1882–1883 (2006).
10. C. C. Winterbourn, Reconciling the chemistry and biology of reactive oxygen species. *Nat. Chem. Biol.* **4**, 278–286 (2008).
11. C. Gorrini, I. S. Harris, T. W. Mak, Modulation of oxidative stress as an anticancer strategy. *Nat. Rev. Drug Discov.* **12**, 931–947 (2013).
12. M. Schieber, N. S. Chandel, ROS function in redox signaling and oxidative stress. *Curr. Biol.* **24**, R453–R462 (2014).
13. D. Trachootham, J. Alexandre, P. Huang, Targeting cancer cells by ROS-mediated mechanisms: A radical therapeutic approach? *Nat. Rev. Drug Discov.* **8**, 579–591 (2009).
14. S. L. Cramer *et al.*, Systemic depletion of L-cyst(e)ine with cyst(e)inase increases reactive oxygen species and suppresses tumor growth. *Nat. Med.* **23**, 120–127 (2017).
15. X. Tang *et al.*, Cystine addiction of triple-negative breast cancer associated with EMT augmented death signaling. *Oncogene* **36**, 4235–4242 (2017).
16. J. B. Kohl, A. T. Mellis, G. Schwarz, Homeostatic impact of sulfite and hydrogen sulfide on cysteine catabolism. *Br. J. Pharmacol.* **176**, 554–570 (2019).
17. M. R. Sullivan *et al.*, Quantification of microenvironmental metabolites in murine cancers reveals determinants of tumor nutrient availability. *eLife* **8**, e44235 (2019).
18. E. C. Lien, L. Ghisolfi, R. C. Geck, J. M. Asara, A. Toker, Oncogenic PI3K promotes methionine dependency in breast cancer cells through the cystine-glutamate antiporter xCT. *Sci. Signal.* **10**, eaao6604 (2017).
19. C. Szabó, Hydrogen sulphide and its therapeutic potential. *Nat. Rev. Drug Discov.* **6**, 917–935 (2007).
20. J. L. Wallace, R. Wang, Hydrogen sulfide-based therapeutics: Exploiting a unique but ubiquitous gasotransmitter. *Nat. Rev. Drug Discov.* **14**, 329–345 (2015).
21. R. Wang, Physiological implications of hydrogen sulfide: A whiff exploration that blossomed. *Physiol. Rev.* **92**, 791–896 (2012).
22. A. K. Mustafa *et al.*, H_2S signals through protein S-sulfhydration. *Sci. Signal.* **2**, ra72 (2009).
23. R. Greiner *et al.*, Polysulfides link H_2S to protein thiol oxidation. *Antioxid. Redox Signal.* **19**, 1749–1765 (2013).
24. T. Ida *et al.*, Reactive cysteine persulfides and S-polythiolation regulate oxidative stress and redox signaling. *Proc. Natl. Acad. Sci. U.S.A.* **111**, 7606–7611 (2014).
25. P. Nagy, Mechanistic chemical perspective of hydrogen sulfide signaling. *Methods Enzymol.* **554**, 3–29 (2015).

26. P. K. Yadav *et al.*, Biosynthesis and reactivity of cysteine persulfides in signaling. *J. Am. Chem. Soc.* **138**, 289–299 (2016).
27. T. Nakamura, Y. Yamaguchi, H. Sano, Plant mercaptopyruvate sulfurtransferases: Molecular cloning, subcellular localization and enzymatic activities. *Eur. J. Biochem.* **267**, 5621–5630 (2000).
28. T. Akaike *et al.*, Cysteinyl-tRNA synthetase governs cysteine polysulfidation and mitochondrial bioenergetics. *Nat. Commun.* **8**, 1177 (2017).
29. É. Dóka *et al.*, Control of protein function through oxidation and reduction of persulfidated states. *Sci. Adv.* **6**, eaax8358 (2020).
30. B. D. Paul, S. H. Snyder, H_2S signalling through protein sulfhydration and beyond. *Nat. Rev. Mol. Cell Biol.* **13**, 499–507 (2012).
31. É. Dóka *et al.*, A novel persulfide detection method reveals protein persulfide- and polysulfide-reducing functions of thioredoxin and glutathione systems. *Sci. Adv.* **2**, e1500968 (2016).
32. J. Zivanovic *et al.*, Selective persulfide detection reveals evolutionarily conserved antiaging effects of S-sulfhydration. *Cell Metab.* **30**, 1152–1170.e13 (2019).
33. R. M. Branca *et al.*, HiRIEF LC-MS enables deep proteome coverage and unbiased proteogenomics. *Nat. Methods* **11**, 59–62 (2014).
34. H. J. Johansson *et al.*, Consortia Oslo Breast Cancer Research Consortium (OSBREAC), Breast cancer quantitative proteome and proteogenomic landscape. *Nat. Commun.* **10**, 1600 (2019).
35. M. R. Aure *et al.*, Oslo Breast Cancer Research Consortium (OSBREAC), Integrated analysis reveals microRNA networks coordinately expressed with key proteins in breast cancer. *Genome Med.* **7**, 21 (2015).
36. M. R. Aure *et al.*, OSBREAC, Integrative clustering reveals a novel split in the luminal A subtype of breast cancer with impact on outcome. *Breast Cancer Res.* **19**, 44 (2017).
37. Cancer Genome Atlas Network, Comprehensive molecular portraits of human breast tumours. *Nature* **490**, 61–70 (2012).
38. L. Silwal-Pandit *et al.*, The longitudinal transcriptional response to neoadjuvant chemotherapy with and without bevacizumab in breast cancer. *Clin. Cancer Res.* **23**, 4662–4670 (2017).
39. C. W. Pugh, P. J. Ratcliffe, Regulation of angiogenesis by hypoxia: Role of the HIF system. *Nat. Med.* **9**, 677–684 (2003).
40. A. L. Harris, Hypoxia—A key regulatory factor in tumour growth. *Nat. Rev. Cancer* **2**, 38–47 (2002).
41. K. J. Briggs *et al.*, Paracrine induction of HIF by glutamate in breast cancer: EglN1 senses cysteine. *Cell* **166**, 126–139 (2016).
42. S. Ros *et al.*, Functional metabolic screen identifies 6-phosphofructo-2-kinase/fructose-2,6-biphosphatase 4 as an important regulator of prostate cancer cell survival. *Cancer Discov.* **2**, 328–343 (2012).
43. D. Peralta *et al.*, A proton relay enhances H2O2 sensitivity of GAPDH to facilitate metabolic adaptation. *Nat. Chem. Biol.* **11**, 156–163 (2015).
44. B. R. Stockwell *et al.*, Ferroptosis: A regulated cell death nexus linking metabolism, redox biology, and disease. *Cell* **171**, 273–285 (2017).
45. S. Singh, D. Padovani, R. A. Leslie, T. Chiku, R. Banerjee, Relative contributions of cystathionine beta-synthase and gamma-cystathionase to H2S biogenesis via alternative trans-sulfuration reactions. *J. Biol. Chem.* **284**, 22457–22466 (2009).
46. J. M. Fukuto *et al.*, Biological hydropersulfides and related polysulfides—A new concept and perspective in redox biology. *FEBS Lett.* **592**, 2140–2152 (2018).
47. V. Kožich *et al.*, Metabolism of sulfur compounds in homocystinurias. *Br. J. Pharmacol.* **176**, 594–606 (2019).
48. A. G. Cox, C. C. Winterbourn, M. B. Hampton, Measuring the redox state of cellular peroxiredoxins by immunoblotting. *Methods Enzymol.* **474**, 51–66 (2010).
49. M. Gao *et al.*, Role of mitochondria in ferroptosis. *Mol. Cell* **73**, 354–363.e3 (2019).
50. A. Papapetropoulos *et al.*, Hydrogen sulfide is an endogenous stimulator of angiogenesis. *Proc. Natl. Acad. Sci. U.S.A.* **106**, 21972–21977 (2009).
51. C. Szabo *et al.*, Tumor-derived hydrogen sulfide, produced by cystathionine-β-synthase, stimulates bioenergetics, cell proliferation, and angiogenesis in colon cancer. *Proc. Natl. Acad. Sci. U.S.A.* **110**, 12474–12479 (2013).
52. B. Szczesny *et al.*, Inhibition of hydrogen sulfide biosynthesis sensitizes lung adenocarcinoma to chemotherapeutic drugs by inhibiting mitochondrial DNA repair and suppressing cellular bioenergetics. *Sci. Rep.* **6**, 36125 (2016).
53. S. Sen *et al.*, Role of cystathionine β-synthase in human breast cancer. *Free Radic. Biol. Med.* **86**, 228–238 (2015).
54. V. Bogdándi *et al.*, Speciation of reactive sulfur species and their reactions with alkylating agents: Do we have any clue about what is present inside the cell? *Br. J. Pharmacol.* **176**, 646–670 (2019).
55. P. Nagy, É. Dóka, T. Ida, T. Akaike, Measuring reactive sulfur species and thiol oxidation states: Challenges and cautions in relation to alkylation-based protocols. *Antioxid. Redox Signal.* **33**, 1174–1189 (2020).
56. A.-T. Mellis *et al.*, The role of glutamate oxaloacetate transaminases in sulfite biosynthesis and H_2S metabolism. *Redox Biol.* **38**, 101800 (2021).
57. A. Dey *et al.*, Cystathione β-synthase regulates HIF-1α stability through persulfidation of PHD2. *Sci. Adv.* **6**, eaaz8534 (2020).
58. N. Krishnan, C. Fu, D. J. Pappin, N. K. Tonks, H2S-Induced sulfhydration of the phosphatase PTP1B and its role in the endoplasmic reticulum stress response. *Sci. Signal.* **4**, ra86 (2011).
59. S. Borowicz *et al.*, The soft agar colony formation assay. *J. Vis. Exp.* **92**, e51998 (2014).
60. J. Krijt *et al.*, Determination of cystathionine beta-synthase activity in human plasma by LC-MS/MS: Potential use in diagnosis of CBS deficiency. *J. Inherit. Metab. Dis.* **34**, 49–55 (2011).
61. Y. Zhu *et al.*, DEqMS: A method for accurate variance estimation in differential protein expression analysis. *Mol. Cell. Proteomics* **19**, 1047–1057 (2020).